



Order–disorder phase transition in the antiperovskite-type structure of synthetic kogarkoite, $\text{Na}_3\text{SO}_4\text{F}$

Margarita S. Avdontceva^a, Andrey A. Zolotarev^a, Sergey V. Krivovichev^{a,b,*}

^a Department of Crystallography, Institute of Earth Sciences, St. Petersburg State University, University Emb. 7/9, 199034 St. Petersburg, Russia

^b Institute of Silicate Chemistry, Russian Academy of Sciences, Makarova Emb. 6, 199034 St. Petersburg, Russia

ARTICLE INFO

Article history:

Received 5 January 2015

Received in revised form

20 July 2015

Accepted 22 July 2015

Available online 23 July 2015

Keywords:

Antiperovskite

Phase transition

X-Ray diffraction

Kogarkoite

Order-disorder

Structural complexity

ABSTRACT

High-temperature phase transition of synthetic kogarkoite, $\text{Na}_3\text{SO}_4\text{F}$, has been studied by high-temperature X-ray powder and single-crystal diffraction. The temperature of the phase transition can be estimated as 112.5 ± 12.5 °C. The low-temperature phase, $\alpha\text{-Na}_3\text{SO}_4\text{F}$, at 293 K, is monoclinic, $P2_1/m$, $a = 18.065(3)$, $b = 6.958(1)$, $c = 11.446(1)$ Å, $\beta = 107.711(1)^\circ$, $Z = 12$. The structure contains thirteen symmetrically independent Na sites with coordination numbers varying from 6 to 8, and six independent S sites. The high-temperature β -phase at 423 K is rhombohedral, $R\bar{3}m$, $a = 6.94(1)$, $c = 24.58(4)$ Å, $Z = 9$. The crystal structure of both polymorphs of $\text{Na}_3\text{SO}_4\text{F}$ can be described as a 9R antiperovskite polytype based upon triplets of face-sharing $[\text{FNa}_6]$ octahedra linked into a three-dimensional framework by sharing corners. In the α -modification, the SO_4 tetrahedra are completely ordered and located in the framework cavities. In the β -modification, there are only two symmetrically independent Na atoms in the structure. The main difference between the structures of the α - and β -phases is the degree of ordering of the SO_4 tetrahedra: in the α -modification, they are completely ordered, whereas, in the β -modification, the complete disorder is observed, which is manifested in a number of low-occupied O sites around fully occupied S sites. The phase transition is therefore has an order–disorder character and is associated with the decrease of structural complexity measured as an information content per unit cell [577.528 bits for the low- (α) and 154.830 bits for the high- (β) temperature modifications].

© 2015 Elsevier Inc. All rights reserved.

1. Introduction

Antiperovskites are perovskite-type materials with cations and anions interchanged so that perovskite-type units are built from anion-centered instead of cation-centered octahedra [1]. In recent years, antiperovskites received special attention due to their unique physical properties such as magnetism and ionic conductivity [2–8]. Krivovichev [9] reviewed antiperovskite-type structures in minerals built upon O- and F-centered octahedra, which demonstrated polytypic variety of this kind of materials. Phase transitions and polymorphism in antiperovskites have been studied by a number of authors. Skakle et al. [10] described tetragonal-to-cubic phase transition in $\text{K}_3\text{SO}_4\text{F}$ occurring at 585 °C. In this paper, we investigate high-temperature behavior of $\text{Na}_3\text{SO}_4\text{F}$, a synthetic analog of natural mineral kogarkoite first described by L.N. Kogarko [11] from alkaline rocks of the Lovozero alkaline massif, Kola peninsula, Russia. Later it was found in hot springs deposits at Mt.

Princeton, Colorado [12], and named after the first discoverer of this phase in nature. However, before being found in nature, a sodium fluoride sulfate was described by de Marignac as early as in 1859 [13]. Later it was also reported by Wolters [14].

Pabst et al. [15] and Pabst and Sharp [12] provided preliminary results of crystallographic studies of kogarkoite and demonstrated that it belongs to the monoclinic system with the obvious pseudorhombohedral subcell. Fanfani et al. [16] re-investigated the crystal structure of synthetic kogarkoite and gave the information about structural relations in the $\text{Na}_2\text{SO}_4\text{-NaX}$ system where $\text{X} = \text{F}$ or Cl . The system includes such minerals as sulphohalite, $\text{Na}_6(\text{SO}_4)_2\text{FCl}$ [17], galeite $\text{Na}_{15}(\text{SO}_4)_5\text{F}_4\text{Cl}$ [18], and schairerite $\text{Na}_{21}(\text{SO}_4)_7\text{F}_6\text{Cl}$ [19] with the F/Cl ratios equal to 1:1, 4:1, and 6:1, respectively. Krivovichev [9] demonstrated that the crystal structures of all these minerals are based upon antiperovskite-type frameworks.

Wolters [14] has determined the melting point of the synthetic kogarkoite as 781 °C. He has suggested that the mineral is hexagonal only above 105 °C on the basis of disappearing lines in the mimetic twin crystals of kogarkoite upon heating. However, the true nature of temperature-induced structural transformations of kogarkoite remained unclear and constitutes the purpose of the present study.

* Corresponding author at: Department of Crystallography, Institute of Earth Sciences, St. Petersburg State University, University Emb. 7/9, 199034 St. Petersburg, Russia.

E-mail address: s.krivovichev@spbu.ru (S.V. Krivovichev).

2. Experimental

Synthetic crystals of kogarkoite, $\text{Na}_3\text{SO}_4\text{F}$, were prepared by evaporation from aqueous solutions of sodium sulfate and sodium fluoride at 25 °C. The crystals occur as pseudo-hexagonal transparent plates.

Thermal behavior of synthetic kogarkoite was studied by high-temperature X-ray powder diffraction using a Rigaku Ultima IV ($\text{CuK}\alpha_{1+2}$ radiation, 40 kV/30 mA, Bragg–Brentano geometry, PSD D-Tex Ultra) diffractometer with a high-temperature attachment in the temperature range of 25–700 °C with the 30–40° steps. Thin powder sample of kogarkoite was deposited on a Pt sample holder ($20 \times 12 \times 2 \text{ mm}^3$) from an ethanol suspension. The unit-cell parameters were calculated using the program package Topas 4.2 [20]. It was observed that the diffraction pattern of kogarkoite changed dramatically in between 100 and 125 °C (Fig. 1).

In order to refine the crystal structure of the low-temperature phase (hereinafter α -phase) and to investigate the crystal structure of the high-temperature (β) phase, a suitable crystal of $\text{Na}_3\text{SO}_4\text{F}$ was mounted on a thin glass fiber for the X-ray single-

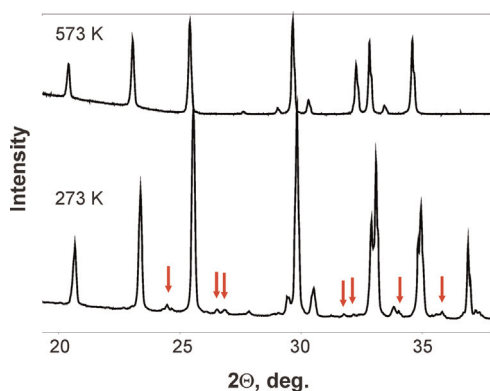


Fig. 1. The diffraction pattern of $\text{Na}_3\text{SO}_4\text{F}$ at 273 and 573 K. Red arrows indicate reflections that are present at 273 K and absent at 573 K. (For interpretation of the references to color in this figure legend, the reader is referred to the web version of this article.)

Table 1
Crystallographic data for synthetic kogarkoite at 293 and 423 K.

Temperature (K)	293	423
Crystal system	Monoclinic	Trigonal
<i>a</i> (Å)	18.064(3)	6.939(9)
<i>b</i> (Å)	6.9578(12)	= <i>a</i>
<i>c</i> (Å)	11.446(2)	24.58(4)
β (deg.)	107.711(4)	90
<i>V</i> (Å ³)	1370.5(4)	1024.96(3)
Space group	$P2_1/m$	$R\bar{3}m$
μ (mm ^{−1})	0.929	0.917
Temperature (K)	293	293
<i>Z</i>	12	9
<i>D</i> _{calc} (g/cm ³)	2.676	2.639
Crystal size (mm ³)	$0.15 \times 0.10 \times 0.09$	$0.15 \times 0.10 \times 0.09$
Radiation	$\text{MoK}\alpha$	$\text{MoK}\alpha$
Total reflections	14818	1850
Unique reflections	3399	355
θ range (deg.)	1.87–28.50	4.98–28.37
Reflections with $ F_o \geq 4s_F$	2483	244
<i>R</i> _{int}	0.0484	0.0689
<i>R</i> _{σ}	0.0461	0.0492
<i>R</i> ₁ ($ F_o \geq 4s_F$)	0.0581	0.0414
<i>wR</i> ₂ ($ F_o \geq 4s_F$)	0.1639	0.1118
<i>R</i> ₁ (all data)	0.0797	0.0664
<i>wR</i> ₂ (all data)	0.1813	0.1230
<i>S</i>	1.073	1.056
$\rho_{\text{min}}, \rho_{\text{max}}, e/\text{Å}^3$	−0.654, 0.154	−0.350, 0.517

crystal diffraction analysis using a Bruker APEX II DUO X-ray diffractometer equipped with the CCD detector at room temperature. More than a hemisphere of X-Ray diffraction data were collected using a microfocus X-ray tube operated with $\text{MoK}\alpha$ radiation at 50 kV and 0.60 mA. The data were integrated using the APEX2 program. The absorption correction was done using a semi-empirical method. The structure was solved in the monoclinic space group $P2_1/m$ by direct methods and refined using least-squares techniques in the SHELXL program [21].

The same crystal was studied using a Oxford Cobra Plus system at 150 °C at the same conditions. Systematic absences of reflections indicated the possible space group $R\bar{3}m$. The structure was solved by direct methods and refined to $R_1 = 0.041$. The refinement showed a strong disorder in the positions of the O atoms of sulfate groups. The lower space groups have been checked, but provided the same results, which pointed out that the phase transition is associated with the disordering of sulfate tetrahedra.

The crystallographic data for the room- and high-temperature modifications of kogarkoite are given in Table 1, the final atomic coordinates and isotropic displacement parameters are given in Tables 2 and 4, respectively, and selected interatomic distances are provided in Tables 3 and 5, respectively. The full list of anisotropic displacement parameters for both phases can be found in the Supplementary information.

Table 2
Atomic coordinates occupancies and isotropic displacement parameters (Å²) of synthetic kogarkoite at 293 K.

Atom	<i>x</i>	<i>y</i>	<i>z</i>	<i>U</i> _{iso}
Na1	1/2	0	1/2	0.019(1)
Na2	0.3508(2)	1/4	0.3033(3)	0.022(1)
Na3	0.1177(2)	1/4	0.8732(2)	0.018(2)
Na4	0.6162(2)	1/4	0.3952(3)	0.020(1)
Na5	0.8530(2)	1/4	0.8161(2)	0.016(1)
Na6	0.3928(2)	1/4	0.9091(3)	0.022(1)
Na7	0	0	0	0.018(1)
Na8	0.8928(2)	1/4	0.4372(2)	0.016(1)
Na9	0.2791(1)	0.0265(3)	0.0317(1)	0.017(1)
Na10	0.4657(1)	0.0180(3)	0.1913(2)	0.019(1)
Na11	0.2453(1)	0.0009(3)	0.7349(2)	0.019(1)
Na12	0.7744(1)	0.0218(3)	0.5509(2)	0.018(1)
Na13	0.9700(1)	0.0229(3)	0.7073(2)	0.017(1)
S1	0.1617(1)	1/4	0.1933(1)	0.009(1)
S2	0.5964(1)	1/4	0.0798(1)	0.013(1)
S3	0.6543(1)	1/4	0.7010(1)	0.010(1)
S4	0.0856(1)	1/4	0.5447(1)	0.011(1)
S5	0.3750(1)	1/4	0.6139(1)	0.010(1)
S6	0.8703(1)	1/4	0.1202(1)	0.009(1)
O1	0.1127(2)	0.0778(5)	0.1799(3)	0.021(1)
O2	0.6457(2)	0.0769(5)	0.0927(3)	0.024(1)
O3	0.6533(2)	0.0769(5)	0.7745(3)	0.025(1)
O4	0.1337(2)	0.0769(5)	0.5536(3)	0.021(1)
O5	0.2012(3)	1/4	0.0992(4)	0.019(1)
O6	0.5597(3)	1/4	0.1782(4)	0.023(1)
O7	0.7241(3)	1/4	0.6624(5)	0.027(1)
O8	0.0484(3)	1/4	0.6416(4)	0.021(1)
O9	0.2198(3)	1/4	0.3164(4)	0.023(1)
O10	0.5365(3)	1/4	0.9602(5)	0.028(1)
O11	0.5842(3)	1/4	0.5948(5)	0.032(1)
O12	0.0246(3)	1/4	0.4234(4)	0.024(1)
O13	0.9179(2)	0.0775(5)	0.1280(3)	0.028(1)
O14	0.8082(3)	1/4	−0.0002(4)	0.021(1)
O15	0.8340(3)	1/4	0.2189(5)	0.027(1)
O16	0.3746(2)	0.07920(6)	0.5376(3)	0.032(1)
O17	0.4424(4)	1/4	0.7213(6)	0.047(2)
O18	0.3045(4)	1/4	0.6502(7)	0.051(2)
F1	0.4807(2)	1/4	0.3576(3)	0.020(1)
F2	0.3778(2)	1/4	0.0961(3)	0.020(1)
F3	0.2394(2)	1/4	0.8644(3)	0.019(2)
F4	0.9909(2)	1/4	0.8755(3)	0.018(1)
F5	0.7438(2)	1/4	0.3933(3)	0.018(1)
F6	0.8754(2)	1/4	0.6270(3)	0.017(1)

3. Results

Fig. 2 shows the behavior of the unit-cell volume of $\text{Na}_3\text{SO}_4\text{F}$ versus temperature (the unit-cell volume of the α -phase was multiplied by the factor of 0.75 in order to conform with that of the β -phase). It can be seen that the unit-cell volume changes dramatically between 100 and 125 °C, which allows to estimate the temperature of the phase transition as 112.5 ± 12.5 °C, well in agreement with the estimates provided by Wolters [14].

The results of the single-crystal structure refinement of α - $\text{Na}_3\text{SO}_4\text{F}$ are in general agreement with those reported by Fanfani et al. [16]. The structure contains thirteen symmetrically independent Na sites with coordination numbers varying from 6 to 8, and six independent S sites. According to [9], the crystal structure of kogarkoite $\text{Na}_3\text{SO}_4\text{F}$ can be described as a 9R perovskite polytype based upon triplets of face-sharing $[\text{FNa}_6]$ octahedra further linked into a three-dimensional framework by sharing corners. The SO_4 tetrahedra are completely ordered and located in the framework cavities (Fig. 3a).

The crystal structure of the high-temperature β -modification of

kogarkoite is based upon the same antiperovskite octahedral framework as observed in the structure of the α -phase (Fig. 3b and c). In contrast, to the low-temperature modification, there are only two symmetrically independent Na in the structure. The main difference between the structures of the α - and β -phases is the degree of ordering of the SO_4 tetrahedra: in the α -modification, they are completely ordered, whereas, in the β -modification, the complete disorder is observed, which is manifested in a number of low-occupied O sites around fully occupied S sites (Fig. 4). The disorder is accompanied by the strong libration effects, which result in the appearance of rather short intrapolyhedral S–O distances (< 1.45 Å) and short intra- and interpolyhedral O–O contacts (< 1.2 and < 2.40 Å, respectively). However, the experimentally obtained short distances are obviously artefacts of the strong thermal disorder observed in the high-temperature modification of synthetic kogarkoite. This observation also points out to the possibility of long-range order that may arise in the intermediate region between the low- and high-temperature crystal structures of kogarkoite, which, however, we were unable to observe in the present study.

4. Discussion

The results of the present study indicate that the temperature-induced α – β transition in $\text{Na}_3\text{SO}_4\text{F}$ is of the order–disorder character. It involves complete disordering of the sulfate tetrahedra, whereas antiperovskite octahedral framework remains basically intact, not taking into account changes in local geometrical

Table 3
Selected bond lengths (Å) in the structure of synthetic kogarkoite at 293 K.

S1–O5	1.463(4)	Na4–F5	2.312(5)	Na12–F5	2.340(3)
S1–O1	1.470(3) 2 ×	Na4–F1	2.353(5)	Na12–F6	2.374(3)
S1–O9	1.479(5)	Na4–O6	2.380(6)	Na12–O7	2.383(4)
< S1–O >	1.471	Na4–O16	2.406(4) 2x	Na12–O9	2.408(3)
		Na4–O11	2.521(6)	Na12–O4	2.423(3)
S2–O10_54	1.464(5)			Na12–O16	2.666(4)
S2–O6	1.471(5)	Na5–F6	2.320(4)	Na12–O18	2.986(7)
S2–O2	1.477(3) 2x	Na5–O1	2.360(3) 2x		
< S2–O >	1.472	Na5–F4	2.375(4)	Na13–F6	2.304(3)
		Na5–O7	2.455(6)	Na13–O1	2.358(4)
S3–O7	1.456(5)	Na5–O14	2.472(5)	Na13–O8	2.391(4)
S3–O11	1.465(5) 2x			Na13–O13	2.413(4)
S3–O3	1.473(4)	Na6–F2	2.238(5)	Na13–F4	2.430(3)
< S3–O >	1.467	Na6–O2	2.377(4) 2x	Na13–O12	2.438(4)
		Na6–O10	2.482(6)		
S4–O8	1.461(5)	Na6–O17	2.568(8)	F1–Na2	2.236(5)
S4–O4	1.471(3) 2x	Na6–F3	2.660(5)	F1–Na1	2.336(2) 2x
S4–O12	1.487(5)	Na6–O18	2.906(8)	F1–Na4	2.353(4)
< S4–O >	1.472			F1–Na10	2.449(3) 2x
		Na7–F4	2.223(2) 2x	< F1–Na >	2.360
S5–O17	1.443(6)	Na7–O13	2.441(4) 2x		
S5–O18	1.455(6)	Na7–O1	2.476(3) 2x	F2–Na6	2.238(5)
S5–O16	1.474(4) 2x			F2–Na10	2.294(3) 2x
< S5–O >	1.462	Na8–F6	2.288(4)	F2–Na9	2.311(3) 2x
		Na8–O4	2.333(3) 2x	F2–Na2	2.562(5)
S6–O13	1.464(4) 2x	Na8–O15	2.399(6)	< F2–Na >	2.334
S6–O15	1.469(5)	Na8–O12	2.434(6)		
S6–O14	1.489(5)	Na8–F5	2.583(5)	F3–Na3	2.233(5)
< S6–O >	1.472			F3–Na11	2.304(3) 2x
		Na9–O3	2.298(4)	F3–Na9	2.400(3) 2x
Na1–F1	2.336(2) 2x	Na9–F2	2.311(3)	F3–Na6	2.660(5)
Na1–O11	2.348(4) 2x	Na9–O2	2.360(4)	< F3–Na >	2.384
Na1–O16	2.492(4) 2x	Na9–O5	2.377(4)		
		Na9–F3	2.400(3)	F4–Na7	2.222(2) 2x
Na2–F1	2.236(5)	Na9–O14	2.443(3)	F4–Na3	2.297(4)
Na2–O9	2.416(6)			F4–Na5	2.375(5)
Na2–O3	2.435(4) 2x	Na10–F2	2.294(3)	F4–Na13	2.429(3) 2x
Na2–F2	2.562(5)	Na10–O6	2.381(4)	< F4–Na >	2.329
Na2–O16	2.844(5) 2x	Na10–O3	2.392(4)		
Na2–O5	2.986(6)	Na10–F1	2.448(3)	F5–Na4	2.312(4)
		Na10–O17	2.495(4)	F5–Na11	2.327(3) 2x
Na3–F3	2.233(4)	Na10–O10	2.538(4)	F5–Na12	2.340(3) 2x
Na3–F4	2.297(4)			F5–Na8	2.583(5)
Na3–O13	2.366(4) 2x	Na11–F3	2.304(3)	< F5–Na >	2.372
Na3–O5	2.565(5)	Na11–F5	2.327(3)		
Na3–O8	2.568(5)	Na11–O2	2.389(4)	F6–Na8	2.288(4)
		Na11–O18	2.391(4)	F6–Na13	2.304(4) 2x
		Na11–O15	2.416(4)	F6–Na5	2.320(4)
		Na11–O4	2.470(4)	F6–Na12	2.374(3) 2x
				< F6–Na >	2.327

Table 4
Atomic coordinates, site-occupation factors (s.o.f.s) and isotropic displacement parameters (Å) of synthetic kogarkoite at 423 K.

Atom	s.o.f.	x	y	z	U_{iso}
Na1	1	1/2	1/2	0	0.051(1)
Na2	1	0.1800(2)	0.3600(3)	0.1089(1)	0.038(1)
S1	1	0	0	0	0.025(1)
S2	1	2/3	1/3	0.1176(1)	0.051(1)
F1	1	1/3	2/3	0.0441(2)	0.051(2)
F2	1	1/3	2/3	1/6	0.037(2)
O1	0.81(1)	0.5520(4)	0.1041(7)	0.0984(2)	0.048(2)
O2	0.81(1)	2/3	1/3	0.1768(2)	0.057(3)
O1A	0.19(1)	0.554(2)	0.109(3)	0.1383(7)	0.043(5)
O2A	0.19(1)	2/3	1/3	0.059(1)	0.070(10)
O3	0.50(2)	0	0	0.0603(1)	0.080(5)
O4	0.30(2)	0.1164(1)	0.233(2)	0.0156(1)	0.046(4)
O5	0.20(2)	0.103(1)	0.206(1)	–0.0299(6)	0.061(1)

Table 5
Selected bond lengths (Å) in the structure of synthetic kogarkoite at 423 K.

S1–O5	1.44(2) 6x	Na1–F1	2.283(4)
S1–O4	1.45(1) 6x	Na1–F1	2.283(4)
S1–O3	1.48(1)	Na1–O4	2.412(9)
S1–O5	1.44(2)	Na1–O2A	2.50(2)
< S1–O >	1.45	Na1–O1	2.493(8)
		Na1–O5	2.55(2)
S2–O1A	1.44(2) 3x		
S2–O2A	1.45(2)	Na2–O1A	2.28(2)
S2–O1	1.46(1)	Na2–F2	2.319(3)
S2–O1A	1.46(1) 3x	Na2–O1	2.342(5)
S2–O2	1.46(1)	Na2–O4	2.42(2)
< S2–O >	1.45	Na2–F1	2.424(5)
		Na2–O2	2.471(6)
		Na2–O1A	2.46(2)
F1–Na1	2.28(1) 3x		
F1–Na2	2.44(1) 3x		
< F1–Na >	2.36		
F2–Na2	2.33(1) 6x		

parameters.

The effect of temperature upon the structural complexity of kogarkoite polymorphs can be estimated using Shannon information content per atom (I_G) and per unit cell ($I_{G,total}$) calculated according to the following formulae [22–24]:

$$I_G = - \sum_{i=1}^k p_i \log_2 p_i \quad (\text{bits/atom}) \quad (1)$$

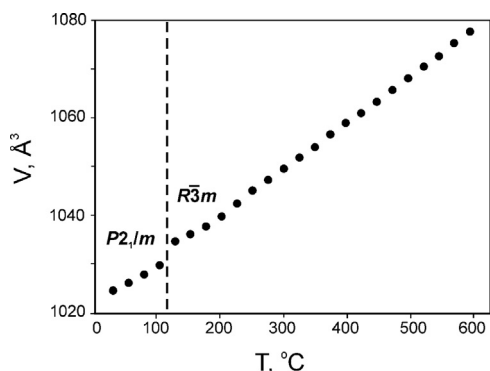


Fig. 2. Temperature dependence of the rhombohedral unit cell volume of $\text{Na}_3\text{SO}_4\text{F}$ versus temperature.

$$I_{G,total} = -\nu I_G = -\nu \sum_{i=1}^k p_i \log_2 p_i \quad (\text{bits/u. c.}) \quad (2)$$

where k is the number of different crystallographic orbits and p_i is the random choice probability for an atom from the i th crystallographic orbit, that is:

$$p_i = m_i/\nu \quad (3)$$

where m_i is a multiplicity of a crystallographic orbit relative to the reduced unit cell, and ν is the number of atoms in the reduced unit cell.

The information-based structural complexity parameters for kogarkoite polymorphs calculated using the Eqs. (1)–(3) are given in Table 6. As it can be seen, the high-temperature phase is structurally simpler than the low-temperature phase, well in agreement with the general trend observed for inorganic crystalline compounds [23]. The temperature-induced decrease in structural complexity is obviously a consequence of the associated increase in both configurational and vibrational entropies.

Table 6
Information-based complexity parameters for two polymorphs of $\text{Na}_3\text{SO}_4\text{F}$.

Polymorph	Space group	ν [atoms]	I_G [bits/atom]	$I_{G,total}$ [bits/unit cell]
α (293 K)	$P2_1/m$	108	5.347	577.528
β (423 K)	$R-3m$	45	3.441	154.830

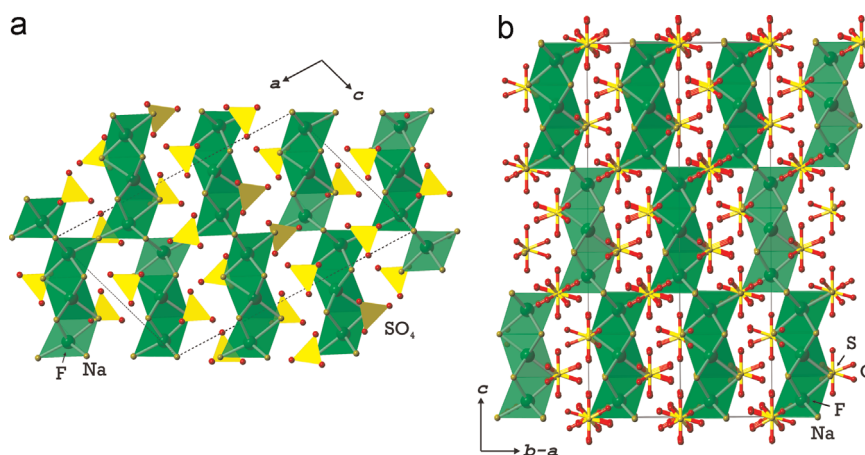


Fig. 3. The crystal structures of $\alpha\text{-Na}_3\text{SO}_4\text{F}$ projected along the b axis (a) and $\beta\text{-Na}_3\text{SO}_4\text{F}$ projected onto (110) plane (b).

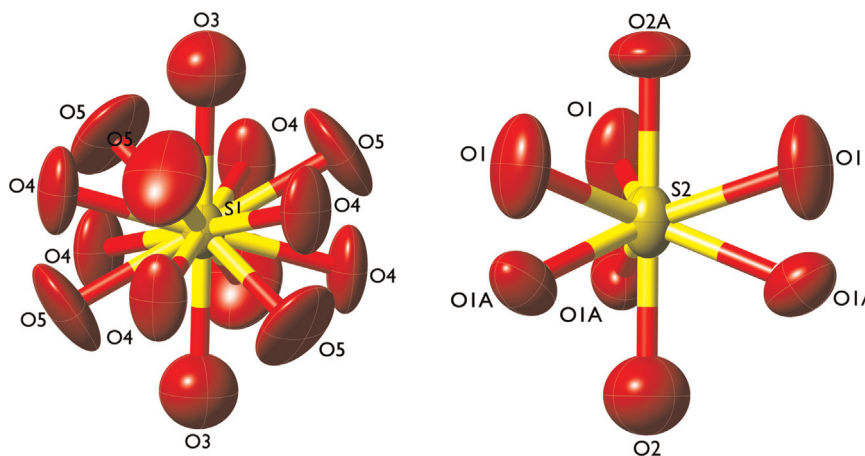


Fig. 4. The arrangements of disordered SO_4 groups in the crystal structure of $\beta\text{-Na}_3\text{SO}_4\text{F}$. Ellipsoids are drawn at 50% probability level.

Acknowledgements

This research was supported by St. Petersburg State University (internal Grant 3.38.136.2014). X-ray diffraction studies were carried out in the SPbSU XRD Resource Centre.

Appendix A. Supplementary material

Supplementary data associated with this article can be found in the online version at <http://dx.doi.org/10.1016/j.jssc.2015.07.033>.

References

- [1] R.H. Mitchell, *Perovskites. Modern and Ancient*, Almaz Press, Thunder Bay, 2002.
- [2] Y. Medkour, A. Roumili, D. Maouche, A. Saoudi, L. Louail, J. Alloys Compd. 541 (2012) 75.
- [3] J. Ramanna, N. Yedukondalu, K. Ramesh Babu, G. Vaitheeswaran, Solid State Sci. 20 (2013) 120.
- [4] Y. Zhang, Y. Zhao, C. Chen, Phys. Rev. B 87 (2013) 134303.
- [5] K. Amara, M. Zemouli, M. Elkeurti, A. Belfedal, F. Saadaoui, J. Alloys Compd. 576 (2013) 398.
- [6] P. Tong, B.-S. Wang, Y.-P. Sun, Chin. Phys. B22 (2013) 067501.
- [7] A. Emly, E. Kioupakis, A. Van der Ven, Chem. Mater. 25 (2013) 4663.
- [8] M.H. Braga, J.A. Ferreira, V. Stockhausen, J.E. Oliveira, A. El-Azab, J. Mater. Chem. A2 (2014) 5470.
- [9] S.V. Krivovichev, Z. Kristallogr. 223 (2008) 109.
- [10] J.M.S. Skakle, J.G. Fletcher, A.R. West, J. Chem. Soc., Dalton Trans. 1996 (1996) 2497.
- [11] L.N. Kogarko, Dokl. Earth Sci. Sec. 139 (1961) 839.
- [12] A. Pabst, W.N. Sharp, Am. Miner. 58 (1973) 116.
- [13] C. de Marignac, Ann. des Mines 15 (1859) 221.
- [14] A. Wolters, N. Jb. Miner. Beil. 30 (1910) 55.
- [15] A. Pabst, D.L. Sawyer, G. Switzer, Am. Miner. 48 (1963) 485.
- [16] L. Fanfani, G. Giuseppetti, C. Tadini, P.F. Zanazzi, Miner. Mag. 43 (1980) 753.
- [17] A. Pabst, Z. Kristallogr. 89 (1934) 514.
- [18] L. Fanfani, A. Nunzi, P.F. Zanazzi, A.R. Zanzari, Miner. Mag. 40 (1975) 357.
- [19] L. Fanfani, A. Nunzi, P.F. Zanazzi, A.R. Zanzari, C. Sabelli, Miner. Mag. 40 (1975) 131.
- [20] A.X.S. Bruker. Topas V4.2: General Profile and Structure Analysis Software for Powder Diffraction Data. Karlsruhe, Germany, 2009.
- [21] G.M. Sheldrick, Acta Crystallogr. A64 (2008) 112.
- [22] S.V. Krivovichev, Acta Crystallogr. A68 (2012) 393.
- [23] S.V. Krivovichev, Miner. Mag. 77 (2013) 275.
- [24] S.V. Krivovichev, Angew. Chem. Int. Ed. 53 (2014) 654.